Supplementary Information

Interplay between spin crossover and proton migration along short strong hydrogen bonds

Verónica Jornet-Mollá, Carlos Giménez-Saiz, Laura Cañadillas-Delgado, Dmitry S. Yufit, Judith A. K. Howard,* and Francisco M. Romero*

Experimental Section

Physical measurements

Magnetic susceptibility measurements were performed using a Quantum Design MPMS-XL-5 magnetometer equipped with a SQUID sensor. Variable temperature measurements were carried out on polycrystalline samples in the temperature range 2-300 K, applying a magnetic field of 1000 Oe. The warming and cooling rates were 0.2 K·min^{-1} between 2 and 20 K and 2.0 K·min^{-1} between 20 and 300 K. The photomagnetic measurements were performed using a thin layer of the compound in order to promote full light penetration. After cooling slowly to 10 K, the sample was irradiated with red light (λ = 630 nm) and the change in magnetisation was followed. Fast saturation of the signal was reached in 10-15 min and irradiation was maintained during 50-100 min. Then, the laser was switched off and the temperature increased at a rate of 0.3 K min^{-1} to determine the *T*(LIESST) value from the minimum of the $\delta(\chi T)/\delta T$ versus *T* curve for the relaxation process.

The relaxation kinetics of the metastable high-spin state has been investigated from 60 to 72 K. First, the photoinduced high-spin phase was achieved by irradiation of the sample at 10 K with a red laser. Then, the sample was warmed while irradiating until the chosen temperature. At this point, the laser was switched off and the time dependence of the magnetic susceptibility recorded in the dark.

Thermogravimetric (TG) measurements were performed under N_2 atmosphere in a Setaram Setsys TGA-ATD16/8 apparatus in the 298-1173 K temperature range at a scan rate of 10 K·min^{-1}.

Differential scanning calorimetry (DSC) analyses were carried out in a Mettler Toledo DSC 821e apparatus and an automated correction from the sample holder was applied. The temperature sweeping rate was 10 K·min^{-1} in order to achieve an adequate signal-to-noise ratio and the measurements were undertaken under N_2 atmosphere.

IR spectra were run on KBr pellets using a Nicolet Avatar 320 FT-IR spectrophotometer in the range 4000-400 cm^{-1} at room temperature. CHN elemental analyses were performed in a CE instruments EA 1110 CHNS analyzer.

Powder X-ray diffraction data were obtained with an Empyrean PANalytical powder diffractometer, using Cu Kα radiation (λ = 1.54056 Å) at room temperature in a 2θ range from 2 to 40°. The simulated diffractogram was obtained from single crystal X-ray data using the CrystalDiffract software.

Synthesis

Ligand bpp was prepared by the previously published procedure.[1] All other reagents and solvents were purchased from commercial sources, with no further purification being undertaken.

$Ba(C_6H_4NO_3)_2 \cdot 4H_2O$

A solution of isonicotinic acid N-oxide (1.046 g, 7.52 mmol) in 40 ml H_2O was combined with a solution of barium hydroxide octahydrate (1.186 g, 3.76 mmol) in 60 ml MeOH. Then, the mixture was refluxed overnight and the resulting solution concentrated using a rotatory evaporator until dryness. The crystalline white product was washed with water and acetone to yield 1.594 g (87 %) of the desired compound. Found: C, 29.42; H, 3.52; N, 5.66. $Ba(C_6H_4NO_3)_2{\cdot}4H_2O$ requires C, 29.68; H, 3.32; N, 5.77. Thermogravimetric analysis confirms the presence of four water molecules in this salt. $\bar{\nu}_{max}/cm^{-1}$: 3394.53, 3108.03, 1598.03, 1545.90, 1390.56, 1225.67, 1177.57, 1139.87, 856.11, 788.13, 685.76, 641.64, 459.14.

$[Fe(bpp)_2](C_6H_4NO_3)_2(C_6H_5NO_3){\cdot}5H_2O$ (**1**)

$FeSO_4{\cdot}7H_2O$ (34.75 mg, 0.125 mmol) was added as a solid to a degassed solution of bpp (53 mg, 0.25 mmol) in 5 ml MeOH yielding a deep red coloured solution after complete dissolution of the metal salt. Then, a solution of $Ba(C_6H_4NO_3)_2{\cdot}4H_2O$ (206.76 mg, 0.426 mmol) in 5 ml H_2O and a suspension of $C_6H_5NO_3$ (17.39 mg, 0.125 mmol) in 1 ml MeOH were added sequentially. After stirring for 2 h at room temperature, the off-white precipitate of $BaSO_4$ was filtered through a low-porosity frit. The filtrate was left undisturbed. Red cubes suitable for X-ray analysis appeared after three days, yielding 74.5 mg (61%). Found: C, 49.01; H, 4.14; N, 18.49. $C_{40}H_{41}FeN_{13}O_{14}$ requires C, 48.84; H, 4.20; N, 18.51. Thermogravimetric analysis confirms the presence of five water molecules in this salt. $\bar{\nu}_{max}/cm^{-1}$: 3366.92, 3232.89, 3108.88, 1611.91, 1413.76, 1374.99, 1360.52, 1248.57, 1222.25, 783.81, 775.40, 635.87.

Deuterated sample (**1d**)

1d was prepared following the same procedure as described for compound **1**, using deuterated solvents (D_2O and CD_3OD) instead of H_2O and CH_3OH. Red cubes were obtained, yielding 67.7 mg (54%). $\bar{\nu}_{max}/cm^{-1}$: 3371.50, 3236.85, 3114.23, 2337.48, 2301.51, 1612.44, 1437.60, 1376.30, 1249.01, 1222.52, 1137.64, 784.33, 775.12, 635.88. Powder X-ray diffraction confirms that **1d** and **1** are isostructural, no other crystal phases being present. IR spectrum shows only partial isotopic exchange. From the ratio of absorbances corresponding to the O–H stretching vibrations in **1** and **1d**, an approximate formula of $\mathbf{1}{\cdot}2.75H_2O{\cdot}2.25D_2O$ was calculated.

X-ray Crystallography

Crystal data were collected on an Oxford Diffraction Supernova diffractometer equipped with a graphite-monochromated Enhance Mo X-Ray Source (λ = 0.71073 Å). Four different single crystals of **1** were coated with Paratone N oil, suspended on a small fiber loop, and cooled in a flow of chilled nitrogen gas at 240 K, 210 K, 120 K and 95 K, respectively. In the last case, the crystal was kept at 95 K during 4 h prior to data collection. Data collection routines, unit cell refinements and data processing were carried out using the CrysAlis software package.[2] Structures were solved using SHELXS-97[3] and refined using SHELXL-2017.[4] The asymmetric unit of **1** at 240 K, 210 K and 95 K contains only one $[Fe(bpp)_2]^{2+}$ cation, five water molecules and three inequivalent isonicotinate N-oxide anions, one of them monoprotonated. At 120 K, there are two independent $[Fe(bpp)_2]^{2+}$ cations, ten water molecules and six inequivalent isonicotinate N-oxide anions, two of them present in their monoprotonated form. In any case, all atoms are lying in general positions. All non-hydrogen atoms were refined anisotropically. H atoms bonded to carbon atoms were included at calculated positions and refined with a riding model. Instead, H atoms of bpp amino groups, all H atoms on water molecules and the hydrogen atom that displays the proton migration (H1O) were found in Fourier difference maps and refined without geometrical restraints. CCDC1873604, CCDC1832988, CCDC1873602 and CCDC1832962 contain the supplementary crystallographic data for **1** at 95 K, 120 K, 210 K and 240 K, respectively. These data are provided free of charge by the Cambridge Crystallographic Data Centre.

Difference Fourier maps (F_o-F_c) were calculated for each temperature on a plane through atoms C29, O1 and O5. All Fourier maps (2×2 Å^2 images) were based on a model produced by removing the hydrogen atom in the short strong hydrogen bond (H1O). On finalising the structure, a LIST 3 command was used and the output structure factors were introduced in the MAPVIEW option in WinGX.[5] The contour level used was 0.1 e·Å^{-3} with a resolution of 0.1 Å.

Neutron Crystallography

The sample was placed on a close-circuit displex device on the monochromatic four-circle diffractometer D19 at ILL (Grenoble, France). The wavelengths used were 1.455 Å and 0.950 Å, provided by a flat Cu monochromator using the 220 and 331 reflections, respectively, at $2\theta_M$ = 69.91° take-off angle. Similar results were obtained with both wavelengths and, accordingly, only the 1.455 Å-data are discussed in the paper. All the measurements were performed with the same single crystal. The sample was cooled down at a cooling rate of 2 K·min^{-1} and data collection was carried out at 240 K, 120 K and 50 K. Additionally, two measurements were done at 95 K and 50 K after complete relaxation of the compound. For both cases, temperature was kept at 95 K for 4 hours in order to achieve complete relaxation prior to data collection at the working temperature. The measurement strategy consisted on 25 omega (ω) scans with steps of 0.07° at different χ and ϕ positions. These omega scans cover either 79° or 64° depending on the χ angle, in order to avoid collisions with the sample environment.

The NOMAD software from ILL was used for data collection. Unit cell determination was done by using PFIND and DIRAX programs, and processing of the raw data was applied using RETREAT and RAFD19 programs.[6] Absorption correction was applied using D19ABS program.[7] All atoms were refined anisotropically without geometrical restraints. CCDC1984961, CCDC1984960, CCDC1984957, CCDC1984959 and CCDC1984958 contain the supplementary crystallographic data for **1** at 240 K, at 120 K, at 50 K and **1** at 95 K and at 50 K after full relaxation to the LS state, respectively.

Variable temperature neutron diffraction experiments for **1** were performed on the Cylindrical CCD Laue Octogonal Photo Scintillator (CYCLOPS), a Laue single-crystal diffractometer at the ILL, Grenoble. Data were collected between room temperature and 10 K, both in the cooling and heating modes. The transition from the HS phase to the mixed-spin phase was reproduced at $T_{\downarrow}$ = 166 K on cooling. Relaxation measurements at 95 K indicated complete conversion to the LS phase after 4 h. Further cooling to 10 K shows the absence of any structural transformation at low temperatures. Upon warming back to room temperature, two crystal phase transitions were observed at approximately 117 K and 166 K, defining the range of stability of the mixed-spin phase. Three movies containing images of Laue patterns corresponding to selected temperatures obtained, respectively, upon cooling, during relaxation and on heating are available in the ESI.

Photocrystallography

Crystal data were collected on a Bruker APEX diffractometer equipped with a graphite-monochromated MoKa radiation (λ = 0.71073 Å). The same single crystal was used for the measurement of the crystal structure of the photoinduced high-spin (PIHS) phase, the structure after partial relaxation of the PIHS phase and the structure obtained from full relaxation of the PIHS state. Compound **1** was cooled until 50 K in a flow of chilled helium with an

Oxford Cryosystems HELIX[8] and, then, was irradiated for 60-90 minutes with a red laser (λ = 630 nm, 5 mW/cm^2) whilst on the diffractometer. After this time, laser irradiation was switched off and data collection started. For the second measurement, after reaching the PIHS state, the sample was warmed to 69 K at 0.3 K·min^{-1} and then quenched at 50 K in order to acquire crystal data of the mixed phase. Finally, the sample was further heated until 95 K and the fully LS phase could be measured. The APEX3 software suite[9] was used for data collection, unit cell determination, data reduction, absorption correction, scaling and space group determination of the collected data. The structures were solved with the SHELXT structure solution program[10] and refined on F^2 using full matrix least-squares methods with the SHELXL-2018[4] software, using Olex2.[11] All non-hydrogen atoms were refined anisotropically. H atoms bonded to carbon atoms were included at calculated positions and refined with a riding model. Instead, H atoms of bpp amino groups, all H atoms on water molecules and the hydrogen atom that displays the proton migration (H1O) were found in Fourier difference maps and refined without geometrical restraints. CCDC1984962, CCDC1984963 and CCDC1984964 contain the supplementary crystallographic data for PIHS **1** at 50 K, **1** at 50 K after partial relaxation and at 95 K upon full relaxation to the LS state, respectively. These data are provided free of charge by the Cambridge Crystallographic Data Centre.

1 Y. Lin and S. A. Lang, *J. Heterocycl. Chem.* 1977, **14**, 345.
2 CrysAlisPro v38.46, Oxford Diffraction Ltd., 2017.
3 G. M. Sheldrick, (1997) SHELXS97. Program for Crystal Structure Solution. University of Gottingen, Gottingen.
4 G. M. Sheldrick, *Acta Cryst*. 2015, **C71**, 3.
5 L. J. Farrugia, *J. Appl. Crystallogr.* 1999, **32**, 837.
6 A. J. M. Duisenberg, *J. Appl. Cryst.* 1992, **25**, 92; G. J. McIntyre and R. F. D. Stansfield, *Acta Cryst.* 1988, **A44**, 257; C. Wilkinson, H. W. Khamis, R. F. D. Stansfield and G. J. McIntyre, *J. Appl. Crystallogr*. 1988, **21**, 471.
7 J. C. Matthewman, P. Thompson and P. J. Brown, *J. Appl. Crystallogr.* 1982, **15**, 167.
8 A. E. Goeta, L. K. Thompson, C. L. Sheppard, S. S. Tandon, C. W. Lehmann, J. Cosier, C. Webster and J. A. K. Howard, *Acta Cryst*. 1999, **C55**, 1243.
9 APEX3 Version 2017.3 (Bruker AXS Inc.)
10 G. M. Sheldrick, *Acta Cryst*. 2015, **A71**, 3.
11 O. V. Dolomanov, L. J. Bourhis, R. J. Gildea, J. A. K. Howard and H. Puschmann, *J. Appl. Cryst*. 2009, **42**, 339.

Table S1. Summary of X-ray crystal data.

	240 K (HS)	**210 K (HS)**	**120 K (HS/LS)**	**95 K (LS)**[b]	**50 K (PIHS)**[c]	**50 K (PIHS$_{rel}$)**[d]	**95 K (LS)**[e]
Formula	$C_{40}H_{41}FeN_{13}O_{14}$	$C_{40}H_{41}FeN_{13}O_{14}$	$C_{40}H_{41}FeN_{13}O_{14}$	$C_{40}H_{41}FeN_{13}O_{14}$	$C_{40}H_{41}FeN_{13}O_{14}$	$C_{40}H_{41}FeN_{13}O_{14}$	$C_{40}H_{41}FeN_{13}O_{14}$
Formula weight	983.71	983.71	983.71	983.71	983.71	983.71	983.71
Crystal system	triclinic	triclinic	triclinic	triclinic	triclinic	triclinic	triclinic
Space group	*P*-1	*P*-1	*P*-1	*P*-1	*P*-1	*P*-1	*P*-1
a/ Å	10.01048(19)	9.99242(16)	13.63358(18)	9.9953(3)	9.9402(13)	9.9614(18)	10.008(4)
b/ Å	13.6732(3)	13.64829(17)	18.8075(2)	13.6057(2)	13.5461(19)	13.577(3)	13.653(7)
c/ Å	17.5596(3)	17.4977(3)	19.6686(2)	17.1602(3)	17.384(2)	17.271(3)	17.130(6)
α/ deg	73.5259(18)	73.5796(13)	64.7142(13)	76.8440(16)	73.959(6)	103.019(8)	76.955(14)
β/ deg	85.7741(15)	85.7654(13)	71.0809(12)	85.770(2)	85.950(5)	94.103(8)	85.823(12)
γ/ deg	69.1588(18)	69.0385(13)	71.0628(12)	110.502(3)	68.735(5)	111.280(7)	110.551(14)
V/Å^3	2153.01(8)	2136.52(6)	4210.47(11)	2098.13(10)	2095.3(5)	2090.1(7)	2105.3(16)
Z	2	2	4	2	2	2	2
T/K	239.9(2)	210.00(14)	120.00(14)	94.9(2)	50(1)	50(1)	95(1)
ρ_{calcd}/g cm^{-3}	1.517	1.529	1.552	1.557	1.559	1.563	1.552
λ/Å	0.71073	0.71073	0.71073	0.71073	0.71073	0.71073	0.71073
θ-range/ deg	2.3410-27.4246	2.4660-27.8098	2.2224-27.7456	2.5480-27.4800	2.200-32.6680	2.202-34.3080	2.199-32.6800
No. of rflns. collected	82160	82858	162319	77954	37908	38146	36767
No. of indep. rflns./*R*int	9117/0.0414	9431/0.0315	18600/0.1052	9155/0.0949	14987/0.0573	15330/0.0585	14901/0.1057
Restraints/ parameters	0/658	0/658	0/1315	0 / 658	0/662	0/658	0 / 658
*R*1/*wR*2 (*I*>2σ(*I*))[a]	0.0328/0.0784	0.0298/0.0720	0.0384/0.1026	0.0459/0.0941	0.0459/0.0999	0.0482/0.1017	0.0632/0.1378
*R*1/*wR*2 (all data)[a]	0.0405/0.0836	0.0350/0.0757	0.0473/0.1125	0.0660/0.1087	0.0803/0.1113	0.0993/0.1156	0.1224/0.1658
$\Delta\rho$max and $\Delta\rho$min/ e·Å^{-3}	0.24/-0.46	0.30/-0.35	0.42/-1.02	0.60/-0.68	0.66/–0.74	0.60/–0.81	1.08/–1.42

[a] $R_1 = \Sigma (Fo - Fc) / \Sigma (Fo)$; $wR_2 = [\Sigma [w(F_o^2 - F_c^2)^2 / \Sigma [w(F_o^2)^2]]^{1/2}$.

[b] Temperature was held at 95 K for 4 h prior to data collection.

[c] Photoinduced high-spin phase.

[d] Structure obtained from partial relaxation of the PIHS phase, then quenching the sample at 50 K.

[e] Structure obtained from full relaxation of the PIHS phase.

Table S2. Atomic displacement parameters (Å^2×10^3) for the different X-ray structures.

Equivalent isotropic displacement parameters, *U*(eq), defined as one third of the trace of the orthogonalised U_{ij} tensor.

atom	**240 K (*HS*)**	**210 K (*HS*)**	**120 K A sublattice (*HS*/LS)**	**120 K B sublattice (HS/*LS*)**	**95 K (*LS*)**[a]	**50 K (PI*HS*)**[b]	**50 K (PIHS$_{rel}$)**[c]	**95 K (*LS*)**[d]
Fe1	22(1)	20(1)	13(1)	12(1)	12(1)	6(1)	8(1)	8(1)
N1	30(1)	28(1)	19(1)	17(1)	16(1)	8(1)	26(1)	12(1)
N2	26(1)	24(1)	17(1)	15(1)	15(1)	7(1)	19(1)	11(1)
N3	25(1)	23(1)	16(1)	15(1)	15(1)	7(1)	15(1)	10(1)
N4	29(1)	27(1)	18(1)	16(1)	16(1)	8(1)	18(1)	11(1)
N5	35(1)	33(1)	21(1)	18(1)	19(1)	9(1)	30(1)	12(1)
N6	29(1)	28(1)	18(1)	17(1)	17(1)	8(1)	17(1)	12(1)
N7	25(1)	23(1)	15(1)	15(1)	14(1)	7(1)	11(1)	10(1)
N8	22(1)	21(1)	14(1)	13(1)	13(1)	6(1)	8(1)	9(1)
N9	25(1)	23(1)	15(1)	14(1)	14(1)	7(1)	13(1)	10(1)
N10	29(1)	26(1)	18(1)	17(1)	17(1)	8(1)	21(1)	12(1)
C1	36(1)	33(1)	23(1)	21(1)	20(1)	10(1)	30(1)	15(1)
C2	34(1)	31(1)	22(1)	19(1)	19(1)	9(1)	24(1)	14(1)
C3	25(1)	24(1)	17(1)	16(1)	15(1)	7(1)	17(1)	11(1)
C4	26(1)	24(1)	17(1)	16(1)	15(1)	7(1)	15(1)	11(1)
C5	32(1)	29(1)	21(1)	19(1)	18(1)	8(1)	17(1)	14(1)
C6	37(1)	33(1)	22(1)	21(1)	21(1)	9(1)	19(1)	16(1)
C7	35(1)	32(1)	22(1)	21(1)	19(1)	9(1)	20(1)	15(1)
C8	27(1)	26(1)	18(1)	16(1)	16(1)	7(1)	16(1)	12(1)
C9	29(1)	27(1)	19(1)	17(1)	17(1)	8(1)	20(1)	13(1)
C10	41(1)	38(1)	25(1)	23(1)	22(1)	10(1)	33(1)	16(1)
C11	44(1)	41(1)	26(1)	23(1)	22(1)	11(1)	41(1)	15(1)
C12	34(1)	32(1)	21(1)	21(1)	19(1)	9(1)	21(1)	15(1)
C13	31(1)	29(1)	19(1)	19(1)	17(1)	9(1)	16(1)	14(1)
C14	24(1)	22(1)	15(1)	15(1)	14(1)	6(1)	9(1)	11(1)
C15	24(1)	22(1)	14(1)	15(1)	13(1)	7(1)	9(1)	10(1)
C16	29(1)	27(1)	18(1)	18(1)	17(1)	8(1)	11(1)	13(1)
C17	32(1)	29(1)	19(1)	19(1)	17(1)	9(1)	11(1)	14(1)
C18	29(1)	26(1)	17(1)	17(1)	16(1)	8(1)	11(1)	13(1)
C19	23(1)	21(1)	14(1)	14(1)	13(1)	7(1)	9(1)	11(1)
C20	24(1)	22(1)	15(1)	14(1)	13(1)	7(1)	10(1)	10(1)
C21	32(1)	29(1)	18(1)	19(1)	18(1)	8(1)	18(1)	14(1)
C22	33(1)	31(1)	21(1)	20(1)	19(1)	9(1)	24(1)	14(1)

N11	36(1)	33(1)	22(1)	24(1)	19(1)	9(1)	12(1)	16(1)
O1	41(1)	37(1)	24(1)	26(1)	20(1)	10(1)	13(1)	17(1)
O2	45(1)	41(1)	29(1)	30(1)	22(1)	11(1)	16(1)	18(1)
O3	52(1)	47(1)	20(1)	21(1)	26(1)	13(1)	16(1)	23(1)
C23	33(1)	30(1)	18(1)	19(1)	17(1)	8(1)	12(1)	14(1)
C24	29(1)	27(1)	18(1)	18(1)	15(1)	7(1)	10(1)	13(1)
C25	33(1)	30(1)	20(1)	20(1)	18(1)	9(1)	13(1)	15(1)
C26	37(1)	33(1)	21(1)	22(1)	19(1)	10(1)	11(1)	15(1)
C27	40(1)	36(1)	23(1)	23(1)	21(1)	10(1)	12(1)	17(1)
C28	36(1)	33(1)	21(1)	21(1)	20(1)	9(1)	14(1)	16(1)
N12	29(1)	26(1)	23(1)	23(1)	15(1)	7(1)	10(1)	13(1)
O4	39(1)	36(1)	28(1)	26(1)	20(1)	10(1)	14(1)	16(1)
O5	51(1)	46(1)	21(1)	22(1)	23(1)	13(1)	16(1)	20(1)
O6	37(1)	34(1)	17(1)	17(1)	19(1)	10(1)	13(1)	16(1)
C29	32(1)	29(1)	19(1)	19(1)	17(1)	8(1)	11(1)	14(1)
C30	28(1)	26(1)	17(1)	18(1)	15(1)	8(1)	10(1)	13(1)
C31	31(1)	28(1)	18(1)	19(1)	16(1)	9(1)	11(1)	14(1)
C32	31(1)	29(1)	19(1)	19(1)	17(1)	9(1)	11(1)	14(1)
C33	32(1)	29(1)	19(1)	19(1)	18(1)	9(1)	12(1)	14(1)
C34	32(1)	29(1)	19(1)	18(1)	16(1)	8(1)	11(1)	14(1)
N13	30(1)	28(1)	25(1)	25(1)	17(1)	8(1)	15(1)	13(1)
O7	45(1)	41(1)	22(1)	22(1)	22(1)	11(1)	18(1)	18(1)
O8	40(1)	36(1)	22(1)	23(1)	20(1)	10(1)	17(1)	16(1)
O9	40(1)	36(1)	18(1)	18(1)	20(1)	10(1)	18(1)	16(1)
C35	31(1)	28(1)	18(1)	18(1)	17(1)	8(1)	14(1)	13(1)
C36	28(1)	25(1)	17(1)	17(1)	15(1)	8(1)	13(1)	12(1)
C37	33(1)	30(1)	19(1)	19(1)	18(1)	9(1)	15(1)	13(1)
C38	34(1)	31(1)	20(1)	20(1)	19(1)	9(1)	16(1)	15(1)
C39	37(1)	33(1)	21(1)	20(1)	19(1)	9(1)	17(1)	16(1)
C40	33(1)	30(1)	20(1)	19(1)	17(1)	9(1)	14(1)	13(1)
O1W	45(1)	40(1)	24(1)	25(1)	22(1)	12(1)	15(1)	19(1)
O2W	47(1)	42(1)	26(1)	29(1)	26(1)	13(1)	17(1)	23(1)
O3W	49(1)	45(1)	29(1)	29(1)	25(1)	13(1)	23(1)	20(1)
O4W	53(1)	48(1)	30(1)	30(1)	29(1)	13(1)	24(1)	23(1)
O5W	63(1)	55(1)	34(1)	33(1)	33(1)	15(1)	19(1)	29(1)
H1O	**106(10)**	**97(9)**	**74(9)**	**83(9)**	**79(13)**	**80(60)/21(12)**	**68(8)**	**61(12)**
H1A	55(7)	54(6)	51(7)	46(7)	42(9)	31(6)	28(6)	33(10)
H1B	68(8)	63(7)	38(6)	37(6)	41(10)	23(6)	27(6)	36(10)
H2A	66(8)	58(7)	35(6)	47(7)	26(8)	48(8)	52(8)	43(11)
H2B	64(8)	59(7)	41(7)	40(7)	45(11)	32(7)	31(6)	51(13)
H3A	61(8)	61(7)	52(7)	51(7)	48(10)	29(7)	55(8)	22(8)

H3B	76(9)	74(8)	38(6)	40(6)	37(10)	33(6)	49(7)	31(9)
H4A	78(10)	71(8)	57(8)	58(8)	49(11)	41(8)	43(7)	39(11)
H4B	84(9)	70(7)	50(7)	51(7)	85(15)	35(7)	39(8)	44(11)
H5A	54(8)	59(7)	40(6)	44(7)	78(14)	23(6)	48(8)	40(10)
H5B	70(8)	60(7)	51(7)	52(7)	41(10)	32(6)	33(7)	33(10)

[a] Temperature was held at 95 K for 4 h prior to data collection.

[b] Photoinduced high-spin phase.

[c] Structure obtained from partial relaxation of the PIHS phase, then quenching the sample at 50 K.

[d] Structure obtained from full relaxation of the PIHS phase.

Table S3. Hydrogen bond distances (Å) for the short strong H-bonds of **1** obtained from X-ray diffraction data at different temperatures.[a]

T **(K)**	***d*** **(O1···H1O) (Å)**	***d*** **(H1O···O5) (Å)**	***D*** **(O1···O5) (Å)**
240	1.12(8)	1.30(8)	2.4247(17)
120[b]	1.33(6)	1.09(6)	2.4216(16)
	1.34(7)	1.09(7)	2.4257(16)
95[c]	1.05(5)	1.38(5)	2.429(2)
50[d]	0.87	1.55	2.420(4)
	1.67	0.77	

[a] Distances measured from Fourier differential maps considering that H1O is located on the maximum of electron density.

[b] The O1···H1O···O5 interaction is split into two: O1A···H1OB···O5B (top line) and O1B···H1OA···O5A (bottom line) due to symmetry breaking.

[c] Temperature was held at 95 K for 4 h prior to data collection.

[d] Photoinduced high-spin phase. Two peaks are observed in the Fourier differential map: H1O1 (top line) and H1O2 (bottom line).

Table S4. Fe–N bond lengths (Å) for **1** at different temperatures obtained from X-ray data.

240 K (*HS*)	**210 K (*HS*)**	**120 K (*HS*/LS)**	**120 K (HS/*LS*)**	**95 K (*LS*)**[a]	**50 K (PI*HS*)**[b]	**50 K (PIHS$_{rel}$)**[c]	**95 K (*LS*)**[d]
Fe1–N2	Fe1–N2	Fe1A–N2A	Fe1B–N2B	Fe1–N2	Fe1–N2	Fe1–N2	Fe1–N2
2.1618(12)	2.1534(11)	2.1539(13)	1.9982(12)	1.9933(19)	2.1541(13)	2.0816(15)	1.996(2)
Fe1–N3	Fe1–N3	Fe1A–N3A	Fe1B–N3B	Fe1–N3	Fe1–N3	Fe1–N3	Fe1–N3
2.1242(12)	2.1167(11)	2.1288(13)	1.9342(13)	1.940(2)	2.1263(13)	2.0384(16)	1.935(2)
Fe1–N4	Fe1–N4	Fe1A–N4A	Fe1B–N4B	Fe1–N4	Fe1–N4	Fe1–N4	Fe1–N4
2.1885(13)	2.1780(11)	2.1781(13)	1.9800(12)	1.9778(19)	2.1889(13)	2.0919(14)	1.971(2)
Fe1–N7	Fe1–N7	Fe1A–N7A	Fe1B–N7B	Fe1–N7	Fe1–N7	Fe1–N7	Fe1–N7
2.1904(13)	2.1822(11)	2.1870(12)	1.9905(12)	1.9921(19)	2.1949(13)	2.1007(14)	1.988(2)
Fe1–N8	Fe1–N8	Fe1A–N8A	Fe1B–N8B	Fe1–N8	Fe1–N8	Fe1–N8	Fe1–N8
2.1152(12)	2.1061(11)	2.1165(12)	1.9380(12)	1.9474(19)	2.1147(13)	2.0343(14)	1.941(2)
Fe1–N9	Fe1–N9	Fe1A–N9A	Fe1B–N9B	Fe1–N9	Fe1–N9	Fe1–N9	Fe1–N9
2.1876(13)	2.1798(11)	2.1880(12)	2.0010(12)	2.0058(19)	2.1908(13)	2.1057(15)	2.0019(19)

[a] Temperature was held at 95 K for 4 h prior to data collection.

[b] Photoinduced high-spin phase.

[c] Structure obtained from partial relaxation of the PIHS phase, then quenching the sample at 50 K.

[d] Structure obtained from full relaxation of the PIHS phase.

Table S5. Octahedral distortion parameters of the Fe^{2+} cations present in **1** at different temperatures obtained from X-ray data.

	240 K Fe1 (*HS*)	**210 K Fe1 (*HS*)**	**120 K Fe1A (*HS*)**	**120 K Fe1B (*LS*)**	**95 K Fe1 (*LS*)**[a]	**50 K Fe1 (PI*HS*)**[b]	**50 K Fe1 ($PIHS_{rel}$)**[c]	**95 K Fe1 (*LS*)**[d]
φ / deg	169.85(5)	169.85(4)	168.13(5)	173.16(5)	172.36(8)	169.10(5)	170.46(5)	172.62(5)
Σ / deg	140.3(6)	139.0(5)	142.0(6)	100.5(6)	103(1)	140.2(6)	123.6(6)	100.2(7)

[a] Temperature was held at 95 K for 4 h prior to data collection.

[b] Photoinduced high-spin phase.

[c] Structure obtained from partial relaxation of the PIHS phase, then quenching the sample at 50 K.

[d] Structure obtained from full relaxation of the PIHS phase.

Table S6. Summary of neutron crystal data.

	240 K (HS)	**120 K (HS/LS)**	**95 K (LS)[b]**	**50 K (HS/LS)**	**50 K (LS)[b]**
Formula	$C_{40}H_{41}FeN_{13}O_{14}$	$C_{40}H_{41}FeN_{13}O_{14}$	$C_{40}H_{41}FeN_{13}O_{14}$	$C_{40}H_{41}FeN_{13}O_{14}$	$C_{40}H_{41}FeN_{13}O_{14}$
Formula weight	983.71	983.71	983.71	983.71	983.71
Crystal system	triclinic	triclinic	triclinic	triclinic	triclinic
Space group	*P*-1	*P*-1	*P*-1	*P*-1	*P*-1
a/ Å	9.9726(3)	13.5877(3)	9.9677(4)	13.5851(9)	9.9719(3)
b/ Å	13.6198(4)	18.7535(5)	13.5502(5)	18.7551(9)	13.5419(4)
c/ Å	17.4815(5)	19.6264(5)	17.0822(5)	19.6424(8)	17.0957(5)
α/ deg	73.5194(17)	64.6623(15)	76.876(2)	64.608(3)	76.716(2)
β/ deg	85.7393(18)	71.0979(17)	85.729(2)	71.048(4)	85.858(2)
γ/ deg	69.1085(18)	71.0863(15)	110.376(2)	71.168(4)	110.386(2)
V/Å^3	2126.23(11)	4174.44(19)	2076.34(13)	4176.3(4)	2076.54(11)
Z	2	4	2	4	2
T/K	240(1)	120(1)	95(1)	50(1)	50(1)
ρ_{calcd}/g cm^{-3}	1.536	1.565	1.573	1.564	1.573
λ/Å	1.455102	1.455102	1.455102	1.4547	1.4547
θ-range/ deg	4.481-60.773	4.510-60.871	4.530-60.800	4.511-60.698	4.527-60.738
No. of rflns. collected	12723	25116	12460	24974	12440
No. of indep. rflns./*R*int	6543/0.0473	12837/0.0428	6404/0.0417	12802/ 0.0435	6336/0.0423
Restraints/ parameters	0/982	0/1963	0/982	0/1963	0/982
$R1$/$wR2$ ($I>2\sigma(I)$)[a]	0.0500/0.1285	0.0639/0.1859	0.0523/0.1358	0.0916/0.3014	0.0782/0.2372
$R1$/$wR2$ (all data)[a]	0.0566/0.1336	0.0761/0.1992	0.0571/0.1400	0.1002/0.3205	0.0807/0.2423
$\Delta\rho$max and $\Delta\rho$min/ e·Å^{-3}	0.66/–0.91	1.50/–1.18	0.93/–1.00	2.694/–2.450	2.024/–1.873

[a] $R_1 = \Sigma (Fo - Fc) / \Sigma (Fo)$; $wR_2 = [\Sigma [w(F_o^2 - F_c^2)^2 / \Sigma [w(F_o^2)^2]]^{1/2}$.

[b] Temperature was held at 95 K for 4 h prior to data collection.

Table S7. Selected H-bond distances (Å) in the crystal structure of **1** at different temperatures obtained from neutron data.

H-bond	**240 K (*HS*)**	**120 K (*HS*/LS)**[a]	**120 K (HS/*LS*)**[b]	**95 K (*LS*)**[c]	**50 K (*HS*/LS)**[a]	**50 K (HS/*LS*)**[b]	**50 K (*LS*)**[c]
N1–H···O3W	1.686(7)	1.666(7)	1.623(7)	1.604(6)	1.652(9)	1.602(9)	1.618(7)
N5–H···O4W	1.828(7)	1.827(8)	1.799(8)	1.785(6)	1.817(9)	1.766(9)	1.797(7)
N6–H···O4	1.802(6)	1.799(6)	1.717(7)	1.728(6)	1.819(9)	1.747(9)	1.725(6)
N10–H···O8	1.661(6)	1.657(6)	1.632(6)	1.660(6)	1.672(8)	1.644(9)	1.654(6)
O1W–H···O6	1.877(8)	1.827(9)	1.850(9)	1.832(8)	1.849(11)	1.879(10)	1.803(9)
O1W–H···O9	1.912(9)	1.882(8)	1.857(8)	1.868(7)	1.903(11)	1.893(11)	1.863(9)
O2W–H···O1W	1.837(8)	1.815(7)	1.793(8)	1.781(7)	1.798(9)	1.789(9)	1.761(7)
O2W–H···O8	1.921(10)	1.913(10)	1.980(10)	1.957(8)	1.916(12)	1.957(11)	1.949(8)
O3W–H···O9	1.934(8)	1.913(8)	1.879(7)	1.873(6)	1.907(8)	1.878(9)	1.890(7)
O3W–H···O2	1.794(7)	1.792(8)	1.746(8)	1.741(7)	1.796(9)	1.735(10)	1.732(8)
O4W–H···O7	1.746(7)	1.738(8)	1.769(8)	1.768(7)	1.751(10)	1.758(10)	1.757(9)
O4W–H···O5W	2.122(11)	2.079(10)	1.901(10)	1.898(8)	2.054(12)	1.887(11)	1.919(10)
O5W–H···O3	1.770(8)	1.777(8)	1.736(8)	1.740(7)	1.792(9)	1.735(9)	1.757(7)
O5W–H···O2W	1.879(8)	1.886(8)	1.850(8)	1.843(7)	1.894(9)	1.852(9)	1.858(8)

[a] Contacts within the A sublattice, except for O1WA–H···O9B, O3WA–H···O9B and O5WA–H···O2WB.

[b] Contacts within the B sublattice, except for O1WB–H···O9A, O3WB–H···O9A and O5WB–H···O2WA.

[c] Temperature was held at 95 K for 4 h prior to data collection.

Table S8. Selected H-bond angles (°) in the crystal structure of **1** at different temperatures obtained from neutron data.

H-bond	**240 K (*HS*)**	**120 K (*HS*/LS)**[a]	**120 K (HS/*LS*)**[b]	**95 K (*LS*)**[c]	**50 K (*HS*/LS)**[a]	**50 K (HS/*LS*)**[b]	**50 K (*LS*)**[c]
N1–H···O3W	167.3(5)	164.1(6)	168.9(6)	166.9(5)	163.1(7)	168.2(7)	167.5(5)
N5–H···O4W	163.2(5)	161.3(6)	153.0(5)	151.2(5)	160.9(7)	152.0(7)	151.1(5)
N6–H···O4	174.3(5)	175.0(5)	166.2(5)	167.3(5)	173.8(7)	166.8(7)	166.5(5)
N10–H···O8	173.3(5)	173.0(5)	170.6(5)	169.7(5)	173.5(6)	170.9(7)	170.6(5)
O1W–H···O6	166.1(6)	166.7(6)	164.6(6)	165.6(5)	165.3(7)	164.4(7)	166.4(6)
O1W–H···O9	161.9(6)	162.7(6)	162.1(6)	162.0(5)	161.3(7)	161.6(7)	162.4(6)
O2W–H···O1W	178.0(6)	177.2(6)	178.9(6)	176.3(5)	175.6(8)	176.8(7)	176.0(6)
O2W–H···O8	173.5(6)	172.2(6)	171.9(6)	172.6(6)	173.1(8)	170.5(7)	172.3(6)
O3W–H···O9	175.1(6)	176.4(6)	174.7(6)	176.2(5)	175.9(8)	173.6(8)	175.7(6)
O3W–H···O2	171.3(6)	172.2(6)	173.1(6)	175.8(6)	173.3(7)	174.1(7)	175.7(6)
O4W–H···O7	170.9(6)	168.3(6)	170.7(7)	169.8(6)	168.1(8)	169.9(9)	170.7(7)
O4W–H···O5W	167.7(7)	167.1(6)	172.8(6)	172.4(6)	173.2(8)	167.0(8)	171.8(7)
O5W–H···O3	178.4(7)	178.1(7)	178.0(7)	178.9(6)	179.2(8)	175.9(8)	179.9(7)
O5W–H···O2W	171.0(7)	169.6(7)	171.5(7)	170.9(6)	171.0(8)	171.1(8)	170.9(7)

[a] Contacts within the A sublattice, except for O1WA–H···O9B, O3WA–H···O9B and O5WA–H···O2WB.

[b] Contacts within the B sublattice, except for O1WB–H···O9A, O3WB–H···O9A and O5WB–H···O2WA.

[c] Temperature was held at 95 K for 4 h prior to data collection.

Table S9. Atomic displacement parameters (Å^2×10^3) for the different neutron structures.

Equivalent isotropic displacement parameters, *U*(eq), defined as one third of the trace of the orthogonalised U_{ij} tensor.

atom	**240 K (*HS*)**	**120 K A sublattice (*HS*/LS)**	**120 K B sublattice (HS/*LS*)**	**95 K (*LS*)[a]**	**50 K A sublattice (*HS*/LS)**	**50 K B sublattice (HS/*LS*)**	**50 K (*LS*)[a]**
Fe1	26(1)	18(1)	15(1)	14(1)	14(1)	12(1)	16(1)
N1	34(1)	24(1)	23(1)	19(1)	19(1)	17(1)	20(1)
N2	30(1)	22(1)	20(1)	18(1)	19(1)	17(1)	19(1)
N3	30(1)	21(1)	20(1)	17(1)	16(1)	15(1)	19(1)
N4	33(1)	23(1)	21(1)	18(1)	17(1)	16(1)	20(1)
N5	39(1)	26(1)	24(1)	20(1)	21(1)	19(1)	22(1)
N6	33(1)	24(1)	22(1)	20(1)	18(1)	18(1)	20(1)
N7	29(1)	20(1)	18(1)	17(1)	17(1)	16(1)	19(1)
N8	27(1)	19(1)	19(1)	16(1)	15(1)	14(1)	20(1)
N9	29(1)	21(1)	20(1)	16(1)	16(1)	15(1)	19(1)
N10	33(1)	23(1)	24(1)	19(1)	18(1)	16(1)	21(1)
C1	39(1)	28(1)	25(1)	21(1)	21(1)	20(1)	21(1)
C2	37(1)	26(1)	25(1)	20(1)	19(1)	18(1)	19(1)
C3	29(1)	20(1)	20(1)	18(1)	15(1)	15(1)	20(1)
C4	29(1)	19(1)	20(1)	17(1)	16(1)	15(1)	19(1)
C5	36(1)	25(1)	25(1)	21(1)	21(1)	20(1)	21(1)
C6	40(1)	27(1)	25(1)	23(1)	21(1)	19(1)	23(1)
C7	38(1)	27(1)	25(1)	22(1)	20(1)	20(1)	22(1)
C8	31(1)	23(1)	21(1)	18(1)	17(1)	18(1)	19(1)
C9	32(1)	21(1)	22(1)	18(1)	17(1)	16(1)	19(1)
C10	44(1)	28(1)	28(1)	22(1)	23(1)	23(1)	22(1)
C11	47(1)	32(1)	28(1)	23(1)	24(1)	21(1)	23(1)
C12	37(1)	24(1)	24(1)	22(1)	18(1)	19(1)	23(1)
C13	35(1)	23(1)	22(1)	19(1)	16(1)	17(1)	21(1)
C14	27(1)	19(1)	18(1)	17(1)	14(1)	13(1)	18(1)
C15	26(1)	19(1)	18(1)	16(1)	15(1)	14(1)	17(1)
C16	33(1)	21(1)	22(1)	19(1)	17(1)	16(1)	20(1)
C17	36(1)	23(1)	24(1)	20(1)	15(1)	16(1)	20(1)
C18	32(1)	21(1)	21(1)	19(1)	17(1)	16(1)	20(1)
C19	26(1)	18(1)	18(1)	16(1)	13(1)	14(1)	18(1)
C20	28(1)	19(1)	19(1)	16(1)	16(1)	15(1)	19(1)
C21	36(1)	23(1)	24(1)	20(1)	17(1)	18(1)	21(1)
C22	37(1)	24(1)	25(1)	20(1)	19(1)	20(1)	22(1)

N11	40(1)	25(1)	25(1)	23(1)	17(1)	17(1)	22(1)
O1	45(1)	25(1)	28(1)	22(1)	19(1)	17(1)	22(1)
O2	49(1)	29(1)	30(1)	26(1)	19(1)	20(1)	24(1)
O3	58(1)	33(1)	34(1)	29(1)	22(1)	22(1)	25(1)
C23	35(1)	22(1)	24(1)	20(1)	16(1)	17(1)	22(1)
C24	32(1)	21(1)	22(1)	19(1)	16(1)	16(1)	21(1)
C25	37(1)	24(1)	24(1)	21(1)	16(1)	18(1)	21(1)
C26	40(1)	24(1)	25(1)	21(1)	18(1)	18(1)	23(1)
C27	43(1)	26(1)	28(1)	23(1)	17(1)	18(1)	22(1)
C28	39(1)	24(1)	25(1)	22(1)	17(1)	18(1)	23(1)
N12	33(1)	21(1)	21(1)	19(1)	16(1)	16(1)	20(1)
O4	43(1)	26(1)	26(1)	22(1)	19(1)	19(1)	22(1)
O5	55(1)	33(1)	30(1)	25(1)	22(1)	20(1)	24(1)
O6	41(1)	25(1)	26(1)	23(1)	19(1)	18(1)	22(1)
C29	35(1)	22(1)	22(1)	20(1)	16(1)	15(1)	20(1)
C30	30(1)	21(1)	21(1)	18(1)	15(1)	15(1)	20(1)
C31	34(1)	20(1)	22(1)	19(1)	15(1)	16(1)	19(1)
C32	34(1)	22(1)	23(1)	21(1)	16(1)	16(1)	20(1)
C33	35(1)	22(1)	24(1)	21(1)	15(1)	17(1)	20(1)
C34	35(1)	23(1)	23(1)	20(1)	16(1)	17(1)	21(1)
N13	35(1)	24(1)	24(1)	20(1)	17(1)	18(1)	22(1)
O7	49(1)	30(1)	28(1)	24(1)	21(1)	21(1)	24(1)
O8	44(1)	28(1)	28(1)	23(1)	20(1)	19(1)	22(1)
O9	44(1)	27(1)	28(1)	23(1)	20(1)	20(1)	21(1)
C35	35(1)	23(1)	22(1)	19(1)	18(1)	16(1)	21(1)
C36	31(1)	20(1)	21(1)	18(1)	16(1)	16(1)	19(1)
C37	37(1)	25(1)	24(1)	19(1)	18(1)	18(1)	21(1)
C38	39(1)	25(1)	24(1)	21(1)	20(1)	18(1)	20(1)
C39	41(1)	27(1)	25(1)	21(1)	21(1)	21(1)	21(1)
C40	37(1)	24(1)	24(1)	19(1)	18(1)	19(1)	20(1)
O1W	47(1)	30(1)	28(1)	24(1)	23(1)	23(1)	24(1)
O2W	51(1)	30(1)	32(1)	26(1)	19(1)	22(1)	25(1)
O3W	51(1)	33(1)	33(1)	26(1)	24(1)	23(1)	26(1)
O4W	56(1)	33(1)	34(1)	30(1)	21(1)	26(1)	26(1)
O5W	66(1)	38(1)	37(1)	34(1)	24(1)	23(1)	31(1)
H1O	**62(2)**	**42(1)**	**48(1)**	**38(1)**	**32(2)**	**34(2)**	**37(1)**
H1A	60(1)	39(1)	46(2)	36(1)	36(2)	34(2)	40(1)
H1B	59(1)	41(1)	36(1)	36(1)	33(2)	31(2)	41(1)
H2A	60(2)	44(2)	44(1)	38(1)	37(2)	35(2)	37(1)
H2B	55(1)	41(1)	47(2)	42(1)	35(2)	29(2)	38(1)
H3A	55(1)	41(1)	38(1)	41(1)	34(2)	32(2)	38(1)

H3B	57(1)	42(1)	40(1)	37(1)	29(2)	35(2)	38(1)
H4A	71(2)	49(2)	46(2)	42(1)	39(2)	42(2)	45(2)
H4B	56(1)	42(1)	43(1)	43(1)	42(2)	36(2)	45(2)
H5A	65(2)	45(2)	43(1)	39(1)	31(2)	35(2)	37(1)
H5B	58(1)	43(1)	42(1)	45(1)	36(2)	34(2)	43(2)

[a] Temperature was held at 95 K for 4 h prior to data collection.

Table S10. Kinetic parameters obtained from relaxation measurements at different temperatures.

T (K)	k_1 (s^{-1})	α_1	k_2 (s^{-1})	α_2
60	$4.4\cdot10^{-5}$	0.9	$4.2\cdot10^{-6}$	0.85
62	$9.6\cdot10^{-5}$	0.87	$1\cdot10^{-5}$	0.55
64	$2\cdot10^{-4}$	0.844	$1.9\cdot10^{-5}$	0.86
66	$3.9\cdot10^{-4}$	0.818	$3.7\cdot10^{-5}$	0.89
68	$6\cdot10^{-4}$	0.79	$7\cdot10^{-5}$	1
70	$9.5\cdot10^{-4}$	0.77	$1.2\cdot10^{-4}$	1.2
72	$2.2\cdot10^{-3}$	0.75	$2.55\cdot10^{-4}$	1

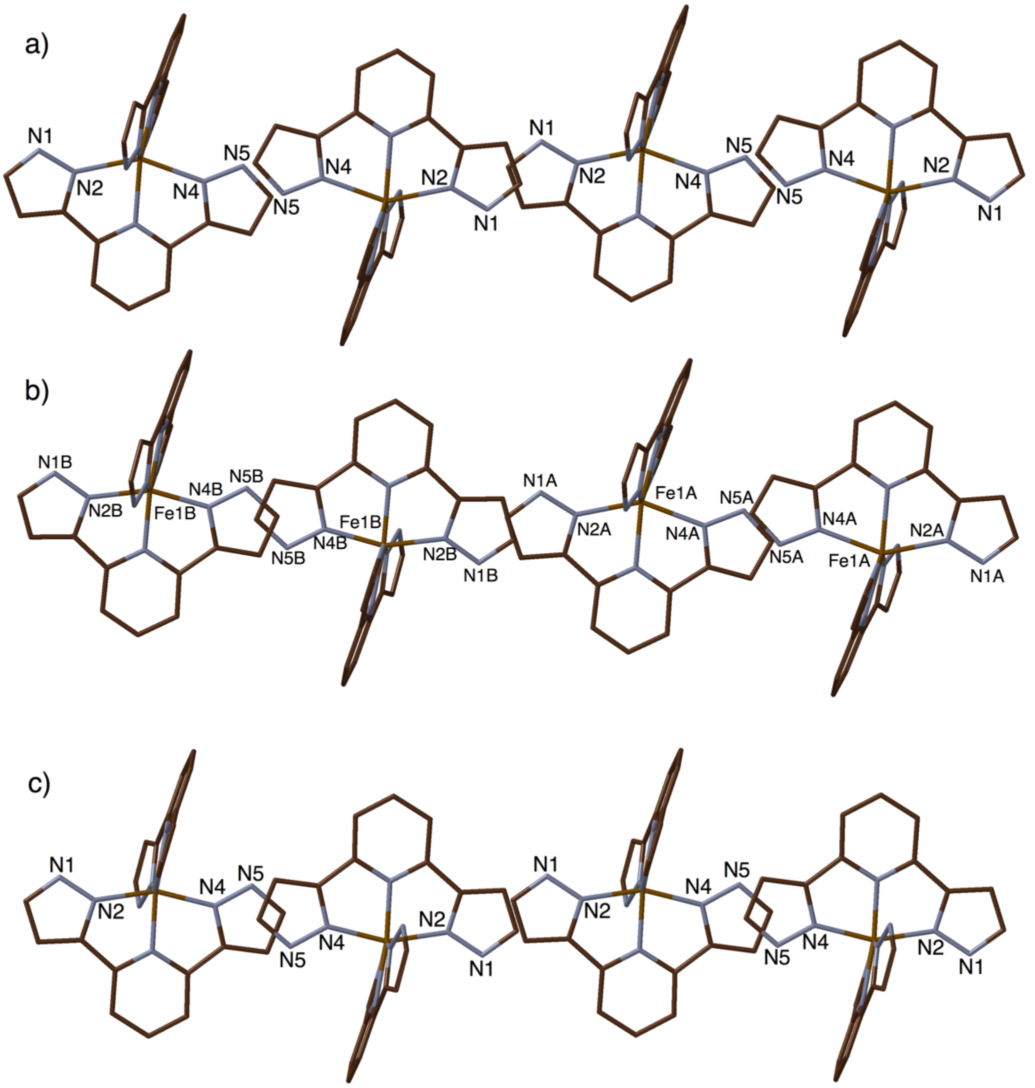

Fig. S1. View of the crystal structure of **1** at 240 K (a), 120 K (b) and 95 K (c) emphasising the presence of π-π stacking interactions to form stacks of $[Fe(bpp)_2]^{2+}$ complexes. Isonicotinate N-oxide anions, H atoms and water molecules are omitted. At 240 K (a), adjacent complexes within the chain are related by a centre of symmetry and thus the two pyrazolyl units involved in the π-π contact lie in strictly coparallel planes. There are two different stacking interactions that alternate along the chain, with interplane distances of 3.390 ± 0.008 Å, corresponding to contacts between N1N2 pyrazole rings, and 3.279 ± 0.008 Å, corresponding to contacts between N4N5 pyrazole rings (here the pyrazolyl units are denoted by the numbering of their N atoms). It is worth noting that the overlapping region in these contacts is small in the first case and almost inexistent in the second, in spite of the closer stacking distance. At 120 K (b), the two independent Fe centres follow an alternating AABB sequence. Now the centre of symmetry located between the N1N2 pyrazolyl units is missing, and the planes containing N1AN2A and N1BN2B are tilted with respect to each other with an angle of 1.325°, leading to a weaker overlap. Instead, the contact between N4N5 pyrazole rings is split into two centrosymmetric interactions: i) between HS centres (N4AN5A rings), being almost identical to that observed at 240 K; ii) between LS centres (N4BN5B rings), showing a stronger overlap. At 95 K (c), the alternated chain structure observed at 240 K, showing only two different centrosymmetric contacts, is restored. The interaction between N4N5 pyrazolyl subunits is much stronger (the overlap region is larger) than those observed at 240 K and 120 K, even between the LS centres. On the contrary, the interaction between N1N2 pyrazolyl subunits weakens with respect to the data measured at 240 K and 120 K, the overlap region being smaller. This is probably due to geometrical constraints introduced by hydrogen bonding and it could be another reason for the high (meta)stability of the intermediate HS/LS state.

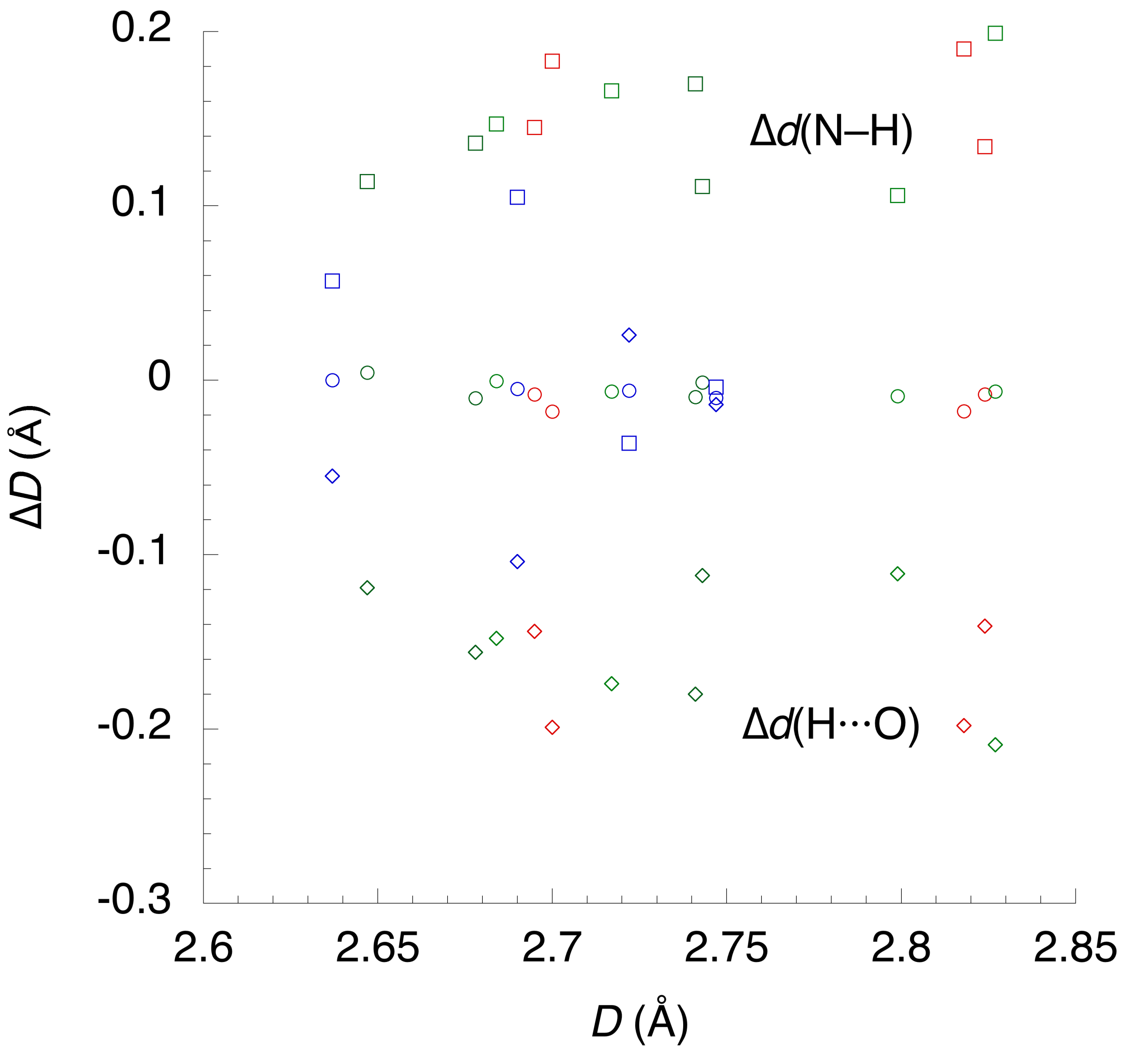

Fig. S2. Comparative plot of H-bonding parameters obtained from neutron (n) and X-ray data. Circles correspond to $\Delta D = (D_n - D_{\text{X-ray}})$, where D is the distance between the heteroatoms. Non-tilted and tilted squares refer, respectively, to Δd(N–H) = (d_n(N–H) – $d_{\text{X-ray}}$(N–H)) and Δd(H···O) = (d_n(H···O) – $d_{\text{X-ray}}$(H···O)). Data have been gathered from measurements at different temperatures: 240 K (red), 120 K (green) and after annealing at 95 K (blue).

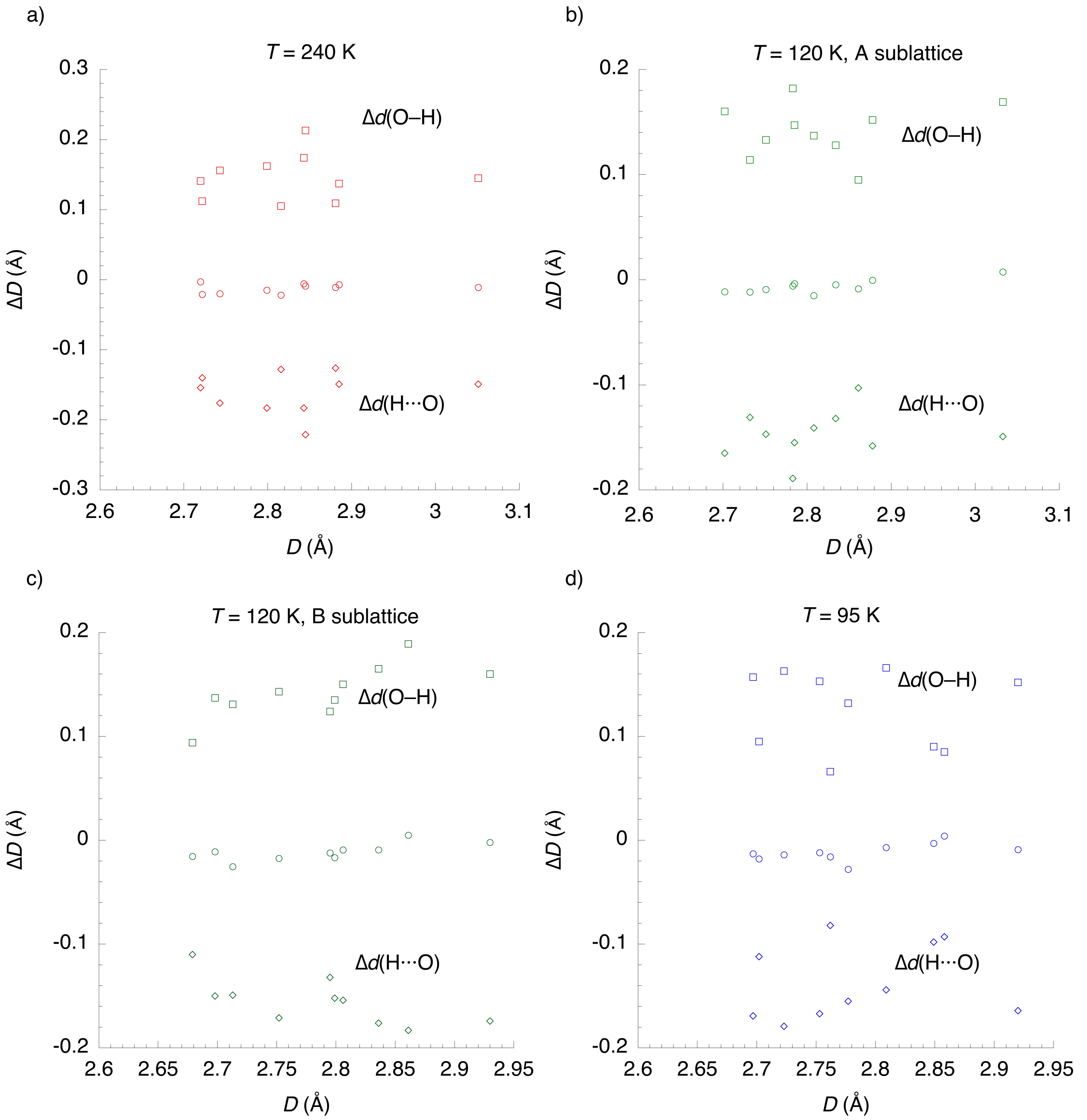

Fig. S3. Comparative plot of H-bonding parameters obtained from neutron (n) and X-ray data. Circles correspond to $\Delta D = (D_n - D_{\text{X-ray}})$, where D is the distance between the heteroatoms. Non-tilted and tilted squares refer, respectively, to $\Delta d(\text{O–H}) = (d_n(\text{O–H}) - d_{\text{X-ray}}(\text{O–H}))$ and $\Delta d(\text{H}\cdots\text{O}) = (d_n(\text{H}\cdots\text{O}) - d_{\text{X-ray}}(\text{H}\cdots\text{O}))$. Data have been gathered from measurements at different temperatures: 240 K (a), 120 K (b, c) and after annealing at 95 K (d).

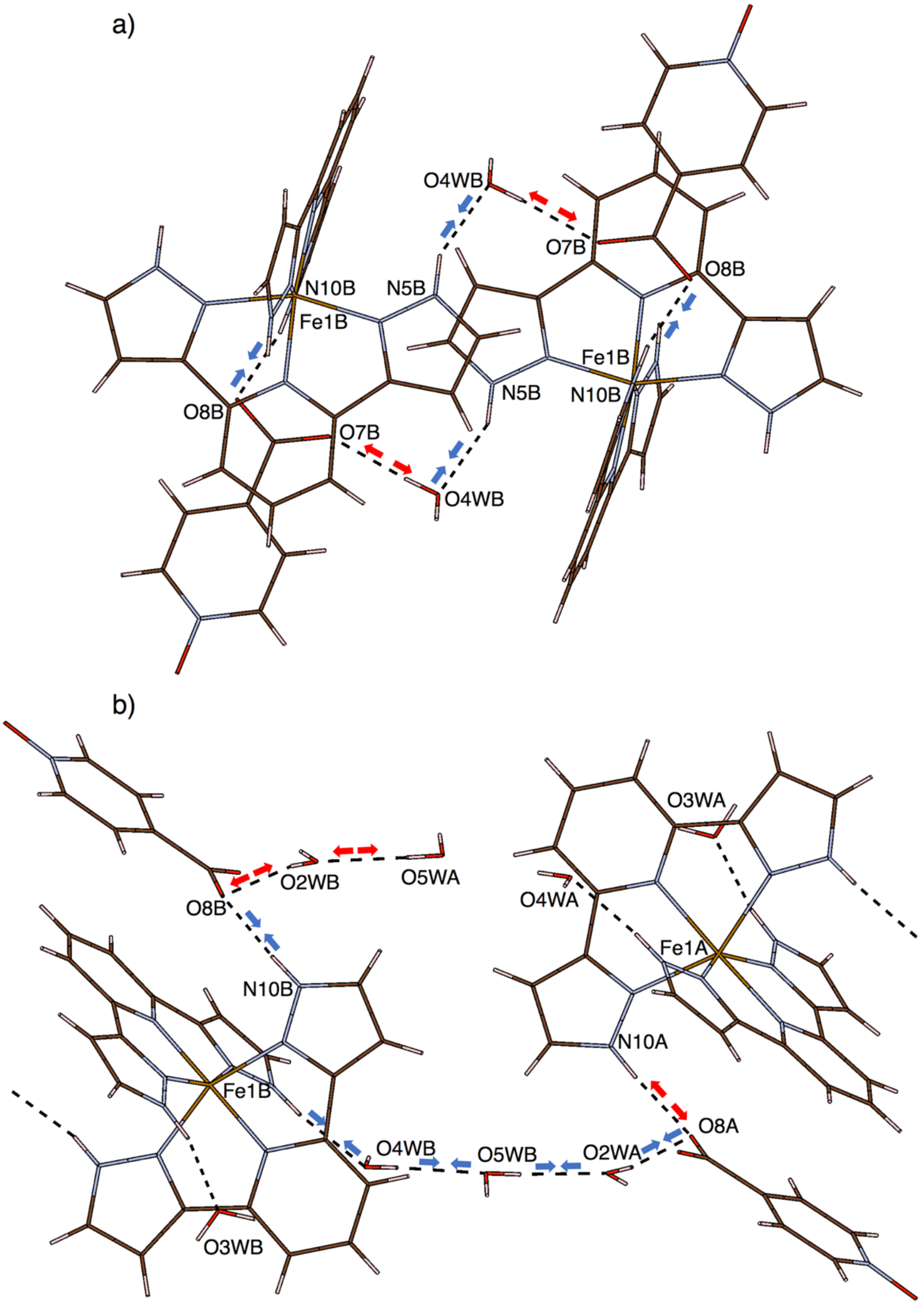

Fig. S4. Crystal structure of **1** in the mixed-spin phase (50% HS, 50% LS) present at 120 K. The view illustrates the importance of H-bond cooperativity in the stabilisation of centrosymmetric LS dimers (a) and the formation of a H-bond between O4WB and O5WB (b). Blue and red arrows refer to decrease and increase of H-bonding distances, respectively.

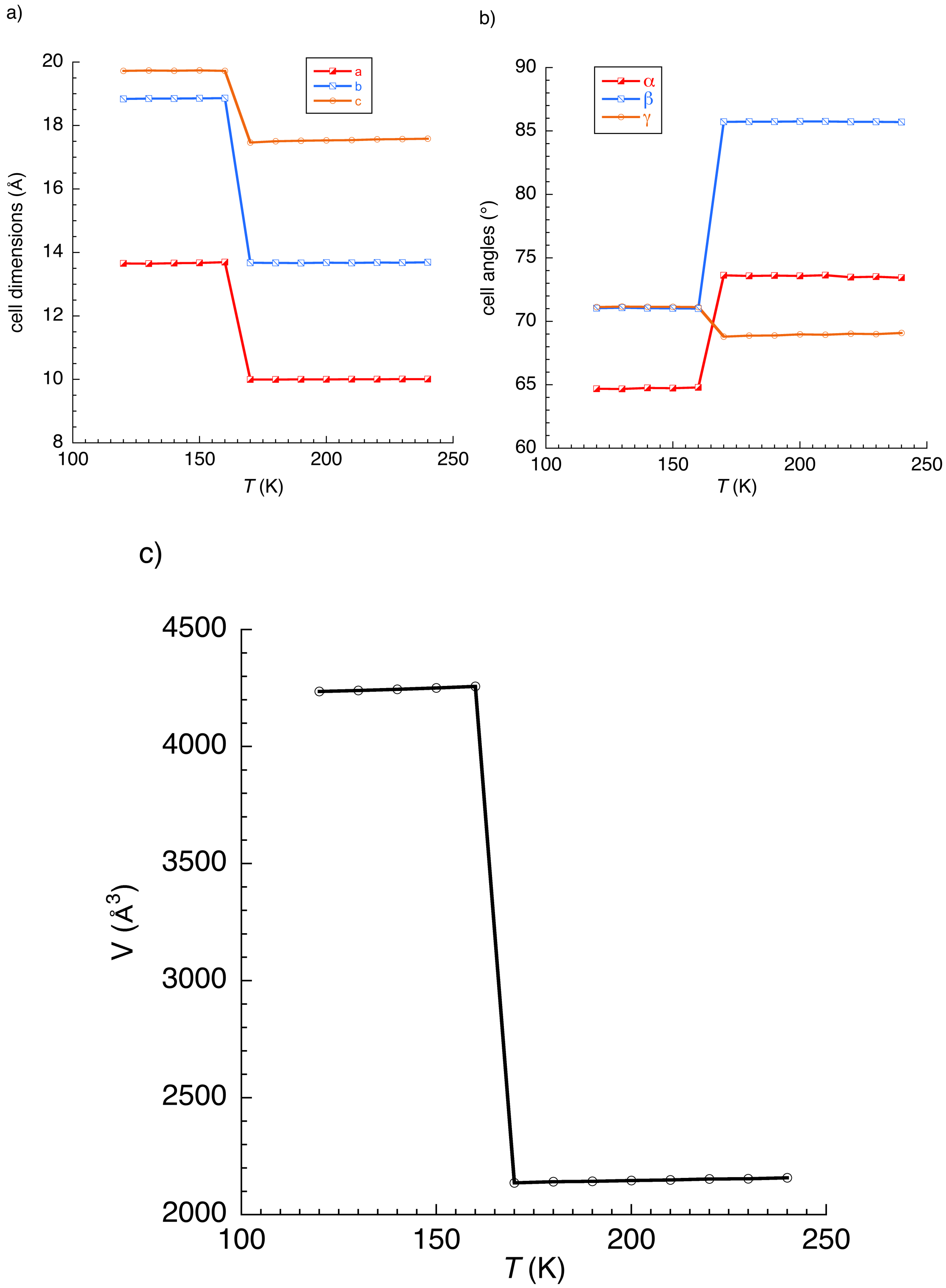

Fig. S5. Temperature dependence of crystal cell dimensions (a), angles (b) and unit cell volume (c) for **1**.

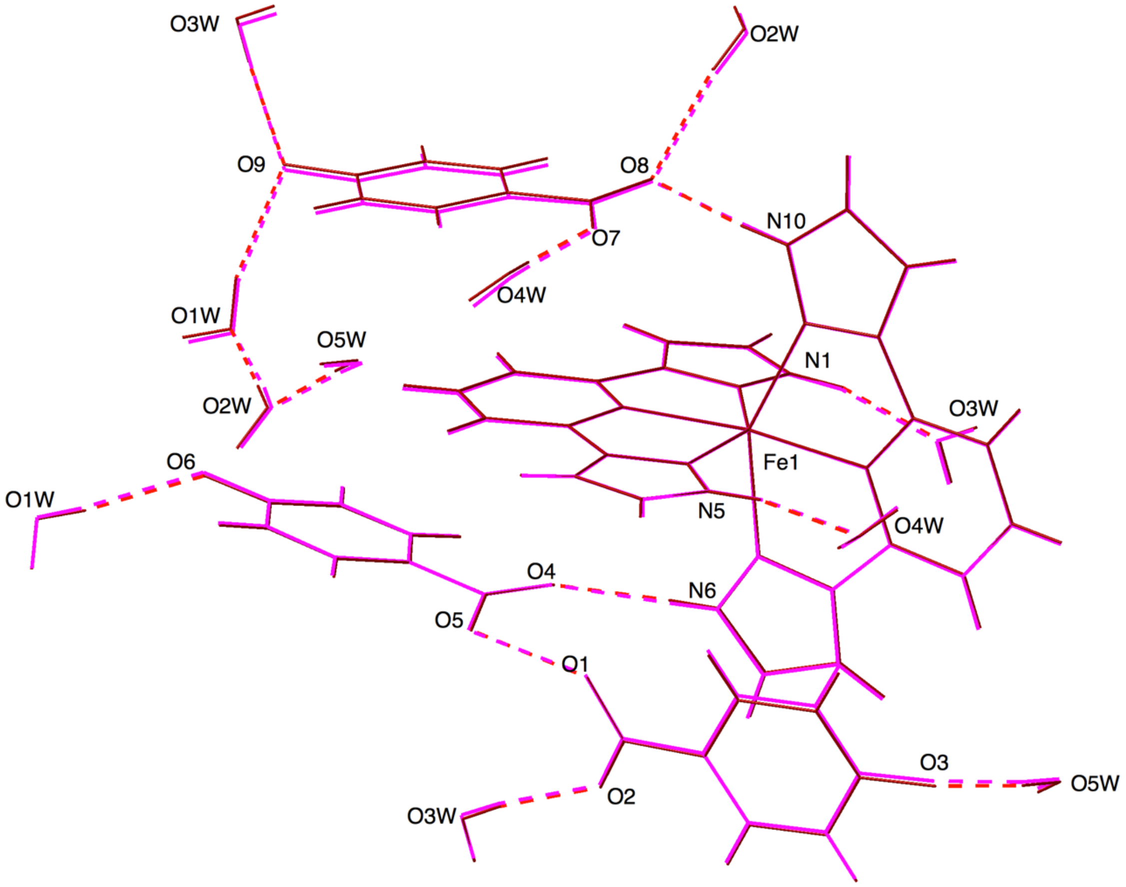

Fig. S6. Superposition of the crystal structures of **1** at 240 K (red) and 50 K (PIHS, magenta) showing the similarity between the thermally stable and photoinduced metastable high-spin phases.

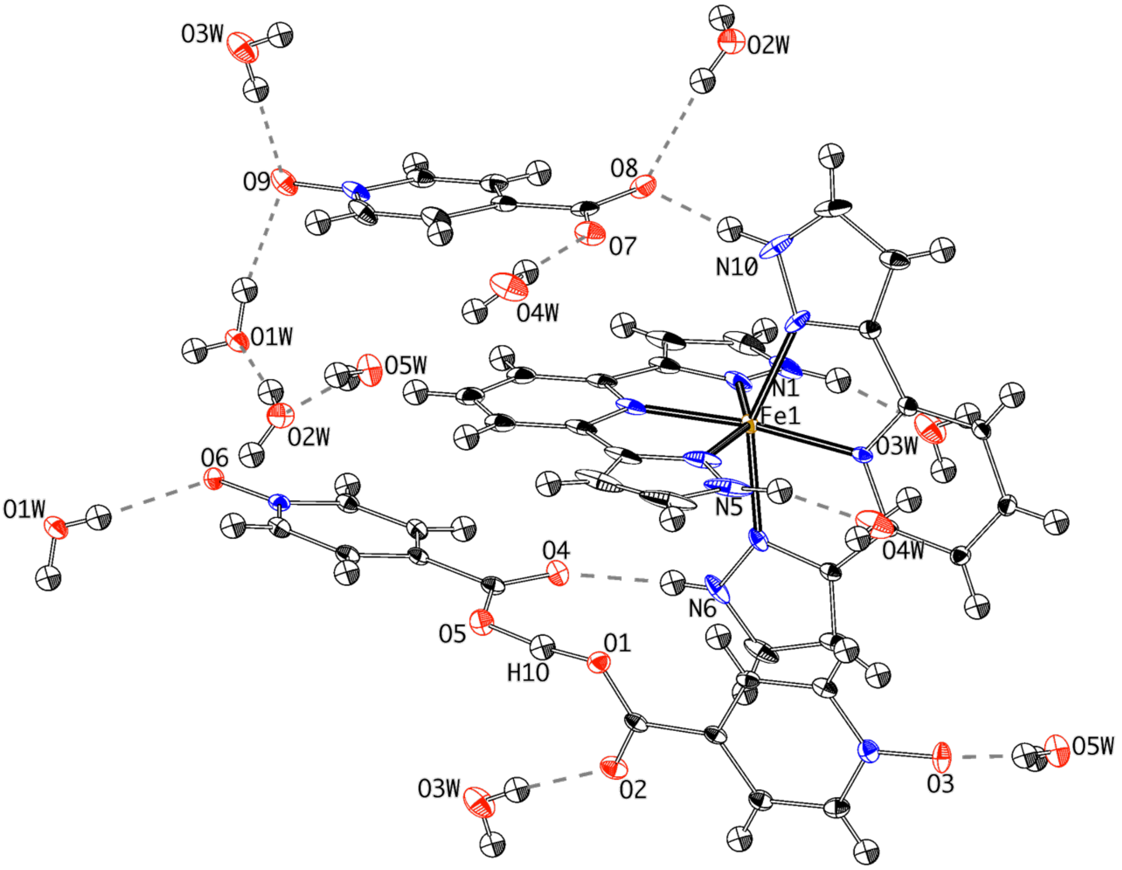

Fig. S7. Thermal ellipsoid plot of the crystal structure of **1** at 50 K after partial relaxation of the photoinduced high-spin phase, showing the hydrogen-bonding connectivity. Note the ellipsoid elongation for those atoms involved in the spin crossover process.

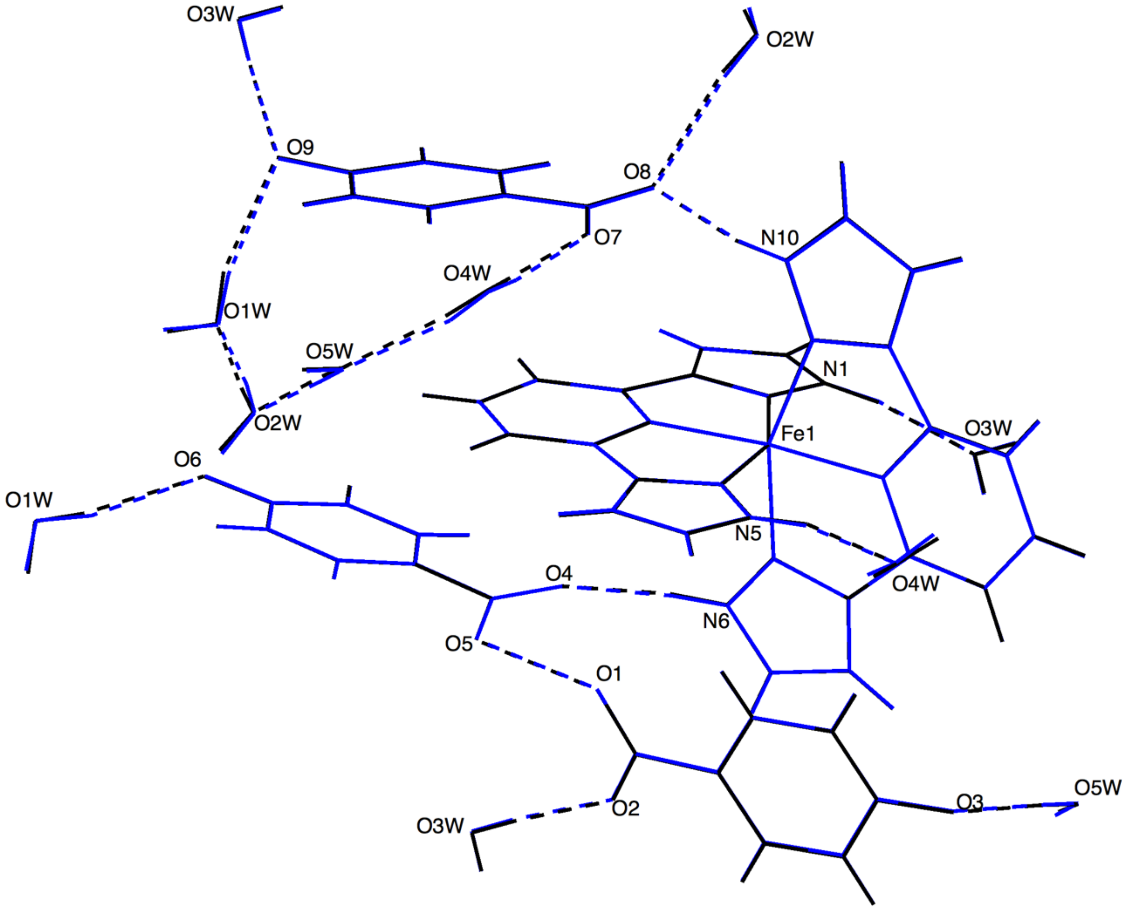

Fig. S8. Superposition of the crystal structures of **1** at 95 K after thermal annealing (blue) and after full relaxation of the photoinduced high-spin phase (black).

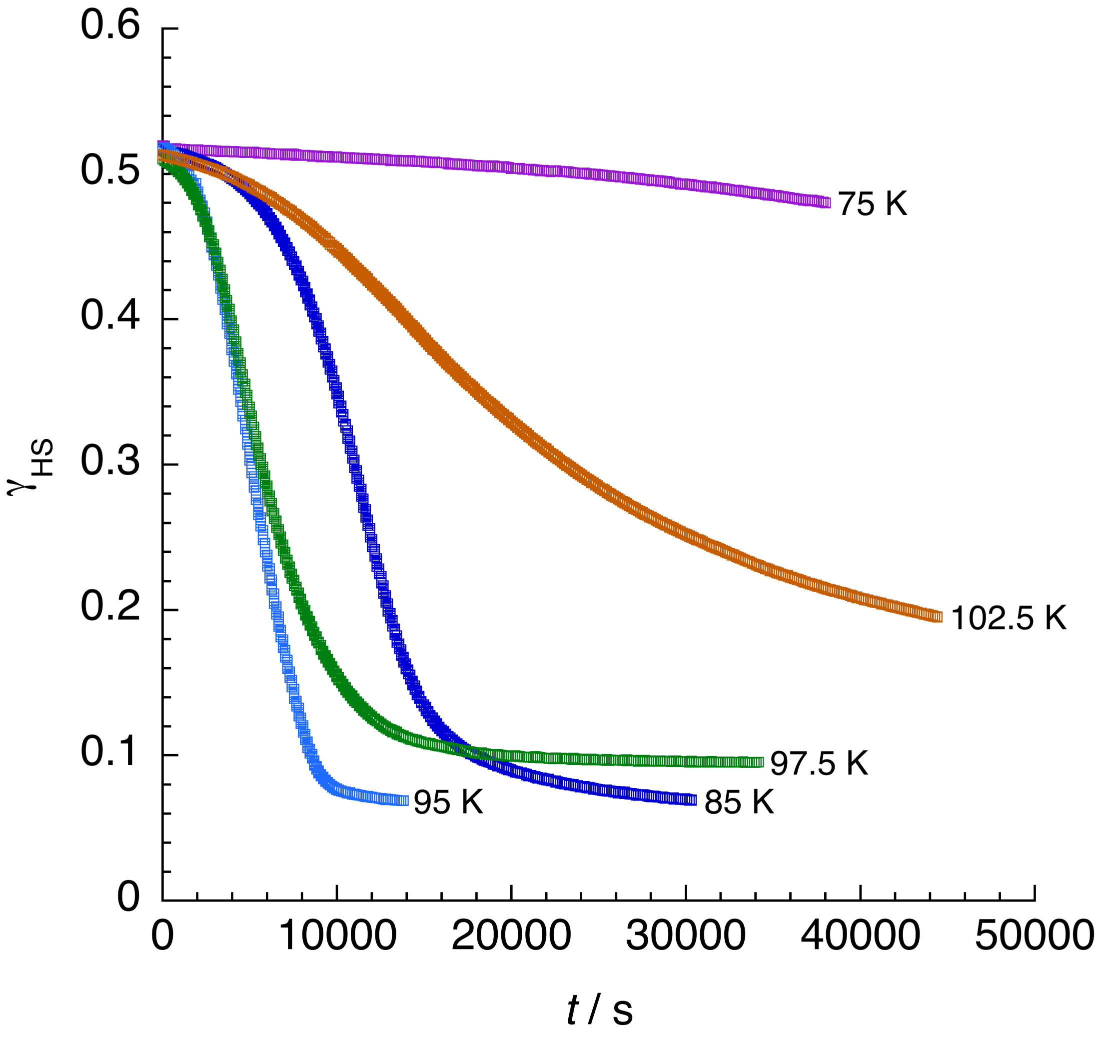

Fig. S9. Time dependence of the fraction of high-spin Fe^{2+} cations of **1** at different temperatures.